Understanding the Evolution of the Pop-out Effect in Si-based Structures for Photovoltaics

E. E. Harea[a,b], K. E. Aifantis[b,c]

[a] *Institute of Applied Physics, ASM, Chisinau, Republic of Moldova,*
[b] *Lab of Mechanics and Materials, Aristotle University, Thessaloniki, Greece,*
[c] *Civil Engineering-Engineering Mechanics, University of Arizona, Tucson, AZ, USA*
e-mail:aifantis@email.arizona.edu

The most interesting phenomenon observed during nanoindentation of Si is the strain burst which occurs during unloading. This feature is referred to as a "pop-out" effect, and it is linked to the phase transformation that occurs underneath the indenter at high stresses. One of the peculiarities of this effect is the observed linear dependence between the depth at which the "pop-out" effect occurs and the maximum penetration depth. By performing a systematic study on the doped Si as well as on photovoltaic structures such as ITO/Si and SnO_2/Si, it is shown that this linearity holds for different unloading rates, which strongly affects the "pop-out" appearance and contact pressure. Furthermore, it is illustrated that that phase transformation in the doped Si is delayed when it is coated with a thin film due to the tension preservation in the imprint under the film coating. This observation suggests that the mechanical properties at the interface between thin films and Si substrates in coated systems (MEMs and photovoltaics) should be further investigated.

Keywords: *pop-out effect, Si, nanoindentation, silicon structures, photovoltaics.*

УДК 538.9:539.2/.6:548.1

INTRODUCTION

One of the most common features observed in load-displacement curves recorded during nanoindentation are strain bursts. Such strain bursts, referred to as "pop-in" effects, take place during loading and indicate dislocation motion [1, 2], or fracture of surface oxides [3, 4]. A peculiar exception to this rule is Si that exhibits a strain burst during unloading [5–9], which is termed a "pop-out". This effect has been widely studied and there are several interpretations for its nature. Pharr [6] attributed the "pop-out" effect to the crystal lateral cracks that are formed under the imprint of the indenter during unloading and can lead to a sudden expulsion of the indenter from Si. However, if this were indeed the case, it can not explain why other materials do not exhibit such strain bursts during unloading.

Another theory, which is more widely accepted, is the emergence of the "pop-out" effect due to a phase transformation that occurs under the indenter [10, 11]. During loading, at pressures between 11.3–12.5 GPa, the density of Si-I increases by 22% and it transforms to Si-II (β-Sn type of structure) [11]. As Si-II is metallic, it has mechanical and electrical properties similar to those of metals. However, this phase is unstable and during unloading it transforms into Si-XII and Si-III, as well as amorphous a-Si. The imprint region, along with the above mentioned crystalline phases, contains some amorphous silicon (a-Si). The mixture of crystalline and amorphous phases in the deformed zone under the imprint depends on the magnitude of the maximum applied load [7, 11 and 12]. At very low loads of ~ 20 mN the amorphous phase is formed predominantly under the indenter, which is shown on the load/displacement curve, $P(h)$, as an "elbow" during unloading, rather than a distinct strain burst. At a maximum applied load of ~ 50 mN, the volume of the mixed amorphous-polycrystalline structures increases. With a further increase of the maximum applied load the quantity of crystalline phases Si-III and Si- XII also increases. In such cases the load/displacement curves $P(h)$ exhibit a distinct "pop-out".

Numerous studies suggest that the final mixture of Si phases during unloading depends not only on the magnitude of the applied load but also on the unloading rate [8, 11, 13–17]. Particularly, it was shown that a slow unloading rate (6–120 mN/min) stimulates the formation of Si-III and Si-XII, while a high unloading rate (> 100 mN/min) favored the formation of the amorphous silicon (a-Si), which strongly affects the occurrence of pop-outs. These works motivated the present study whose purpose is to understand the sensitivity of the indentation depth at which the pop-out occurs to the nanoindentation parameters, such as the maximum applied load, penetration depth, as well as unloading rates. A wide range of maximum loads were examined (20–500 mN), while the loading and unloading rates were either kept constant or varied, between 40–1000 mN/min in order to observe how the depth at which the pop-out occurred would be affected.

It is well known that the mechanical properties in thin film/substrate systems are different from those

of their bulk counterparts. Hence, the question arises regarding the evolution of pop-outs in the coated silicon systems. This is why in addition to testing *n*-Si, coated silicon systems such as ITO/Si and SnO_2/Si used as photovoltaic cells were examined and *n*-Si was coated with a thin film (~ 350 nm) of ITO or SnO_2. These films with significant differences in their mechanical properties (especially adhesion), belong to the class of ceramic materials. The ITO films were our choice because they are used in different devices since they have outstanding physical properties such as: thermal, electrical and chemical stability, adhesion, transparency, thermoelectricity, conductivity, and piezoresistivity. Furthermore, the ITO films are used as transparent contacts for solar cells [18], active elements for temperature measurements [19], pressure sensors [20] and are promising gauge sensors that can work in elevated temperature conditions (up to 1500°C) [21]. So we try to answer some fundamental questions about Si using coated silicon systems that are fabricated for practical applications as solar cells.

EXPERIMENTAL PROCEDURE

Indentation was performed, using the trapezoidal loading sequence on a CSM nanoindenter. The maximum applied load (P_{max}) varied from 20 mN to 500 mN, as shown in Table 1, and a hold time of 20 seconds was used in all cases. Different conditions allowed for the loading/unloading rates were as follows: (i) the loading and unloading rates were taken equal to each other, and were twice the maximum load/minute for each maximum load, (ii) the loading rate varied as in (i) but the unloading rate was kept constant at 80 mN/min (slow rate) for all maximum loads, (iii) the loading rate was varied as in (i) and (ii), but the unloading rate was kept constant at 600 mN/min (high rate) for all maximum loads.

As mentioned in the Introduction, these experiments were repeated for three Si samples: *n*-type Si, ITO/Si, and SnO_2/Si. The structures of ITO/Si and SnO_2/Si are promising for converting solar energy into electricity. These structures were obtained by pyrolytic spraying of the alcoholic solution of indium chloride and tin chloride ($InCl_3$:$SnCl_4$) in the case of ITO films, and the alcoholic solution of tin chloride ($SnCl_4$) in the case of SnO_2 films, on a heated phosphorus doped-silicon substrate, with a (100) crystallographic orientation [22]. As a result, initially a thin layer of SiO_2 of about 3–5 nm formed, followed by a polycrystalline film of In_2O_3:SnO_2 (ITO) or SnO_2, with a ~ 350 nm thickness. Since ITO and SnO_2 have significantly different mechanical properties it is important to investigate how they affect the substrate mechanical behavior during indentation.

The surface roughness is an important parameter that can affect the determination of mechanical parameters during nanoindentation [23]. Based on the atomic force microscopy (AFM) measurements the average roughness for ITO was R_a = 6.4 ± 0.5 nm, and for the SnO_2 film it was R_a = 10.5 ± 1.2 nm. These parameters were taken into consideration during the hardness and elastic modulus measurements (maximum penetration depth was chosen $h_c \approx 50$ nm in accordance with ISO 14577-4, where the surface roughness vs. indentation depth should be $R_a < 5\%$ h_c and $h_c < 10$–15% of the coating thickness).

The hardness and elastic modulus of the samples were automatically calculated by the nanotester software using the Oliver-Pharr method [24].

The adhesive properties of coated systems were assessed using the method proposed by Rosenfeld et al. [25], which is based on the indentation data. The energy (G) necessary to delaminate the coating from the substrate can be determined from the following expression:

$$G = \frac{0.627 H_f^2 t\left(1-\nu_f^2\right)}{E_f\left[1+\nu_f+2\left(1-\nu_f\right)H_f a^2 / P_{max}\right]^2} \qquad (1)$$

where E_f and ν_f are the Young's modulus and Poisson's ratio of the coating, respectively, H_f is the hardness of the coating, a is the measured diameter of the delaminated area, t is the film thickness and P_{max} is the value of the applied load.

RESULTS

Coatings strongly affect the mechanical properties of structures. Figure 1 shows that the maximum penetration depth in Si, ITO/Si and SnO_2/Si structures depends on the maximum applied load.

For SnO_2/Si it can be seen that after P_{max} = 60 mN, its $h_m(P_{max})$ plot is nearly parallel with the $h_m(P_{max})$ curve for the doped Si. This suggests that the SnO_2 volume that is compressed from the indenter deforms until delamination and the circular crack formation occurs at loads between $0 < P_{max} < 60$ mN. The moment at which film delamination takes place can be determined from the large "pop-in" that appears in the load-penetration curves (Fig. 2e and f) [26]. This "pop-in" occurs, since during delamination the bonding forces between the film and the substrate are suddenly broken. Particularly, the film compresses the substrate material around the indenter until delamination, but after delamination it can move easier and form for example pile-ups. Hence, fast lattice reorganization takes place and the indenter tip "falls" into the material at a constant load, resulting in a "pop-in". As the h_{max} vs P_{max} plots for *n*-Si and SnO_2/Si are parallel after delamination in the latter, it can be assumed that for

Table 1. Loading-unloading parameters

P_{max}, mN	Case (i)	Case (ii)		Case (iii)	
	Loading rate=unloading rate, mN/min	Loading rate, mN/min	Unloading rate, mN/min	Loading rate, mN/min	Unloading rate, mN/min
20	40	40	80	40	600
40	80	80		80	
60	120	120		120	
80	160	160		160	
100	200	200		200	
200	400	400		400	
300	600	600		600	
400	800	800		800	
500	1000	1000		1000	

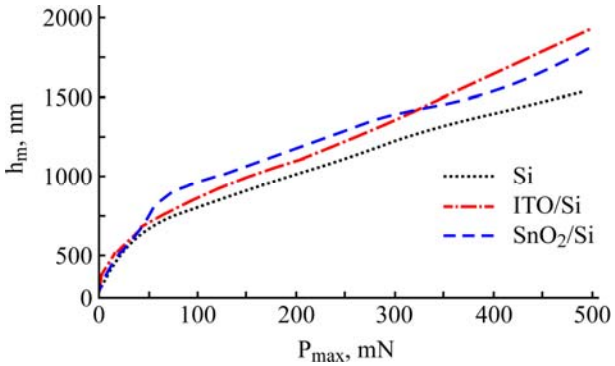

Fig. 1. Maximum penetration depth in Si, ITO/Si and SnO_2/Si structures depending of maximum applied load.

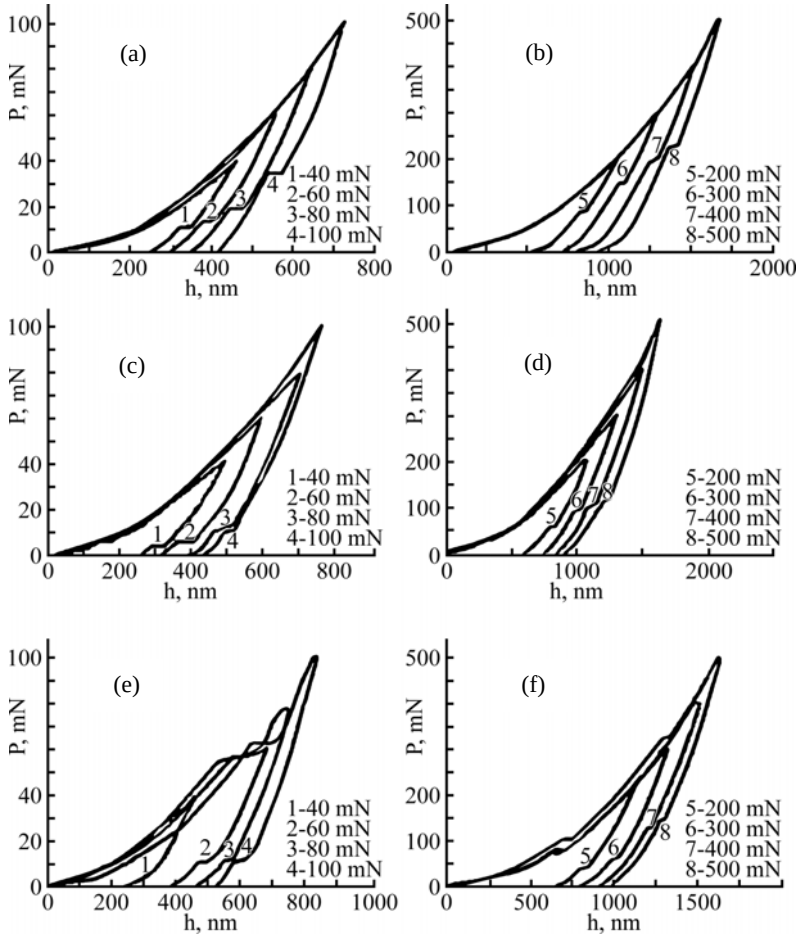

Fig. 2. Load-displacement curves for: (a) and (b) doped Si, (c) and (d) ITO/Si, (e) and (f) SnO_2/Si.

Table 2. $h_{pop\text{-}out}$ (h_m) function constants and mechanical properties determined from nanoindentation and AFM

Material	Constants		Hardness H, GPa	Young's modulus E, GPa	Roughness R_a, nm	Adhesion G, J/m^{-2}
	A	B				
Si	0.88	-72	13.2 ± 0.2	150 ± 10	1.2 ± 0.5	–
ITO	0.88	-123	9.6 ± 0.4	126 ± 16	6.4 ± 0.5	9.5 ± 0.8
SnO_2	0.81	-89.5	7.5 ± 0.3	146 ± 11	10.5 ± 1.2	0.11 ± 0.05

P_{max} > 60 mN, the SnO_2 film consistently affects the penetration of the indenter into the Si substrate regardless of the maximum applied load. It can be supposed that the silicon substrate is indented by a modified indenter system, which is the Berkovich diamond indenter covered by the stretched SnO_2 film. On the other hand, for the ITO/Si structure starting from P_{max} = 40 mN a monotonous increase is observed of the maximum penetration depth versus the maximum applied load in the coated samples compared with the uncoated Si. This suggests that the influence of the ITO film on the mechanical properties of the ITO/Si structure decreases continuously as the maximum applied load increases. This may be due to the fact that as the penetration increases the thickness of the stretched ITO film that covers the Berkovich diamond tip significantly decreases, making the existence of ITO negligible for applied high loads, whereas the thickness of the SnO_2 most likely remained more uniform with penetration depth. In Table 2 it can be seen that the elastic modulus of ITO is lower than that of SnO_2, which suggests that ITO bends more and therefore with increasing indentation depths (applied high loads) the thickness of ITO covering the tip would be less.

The nanoindentation experiments on all tested samples (Si wafers doped with phosphorus, the ITO/Si and SnO_2/Si structures) showed the existence of the anticipated "pop-out" (Fig. 2). The phenomenon had a probabilistic nature and occurred in about 80% of the total number of experiments depending on the unloading rate and applied load. The ITO and SnO_2 films had a significant influence on the emergence and development of the effect.

In the ITO/Si samples the "pop-out" began to appear when the maximum applied load was P_{max} = 40 mN or higher, while in the SnO_2/Si samples it began at loads of P_{max} = 60 mN and higher (Fig. 2). This is directly related to the presence of the ITO or SnO_2 thin film on the Si surface. In the uncoated samples the "pop-out" appeared starting with the load of 20 mN. When the load was not high enough to produce a distinct burst, an "elbow" feature was observed.

The depth at which the "pop-out" occurred ($h_{pop\text{-}out}$) was defined as $(h_1 - h_2)/2+h_2$ (Fig. 3), where h_1 was the depth at which the burst began and h_2 the depth at which it ended. The values of h_m and h_r are the maximum and residual depth, respectively.

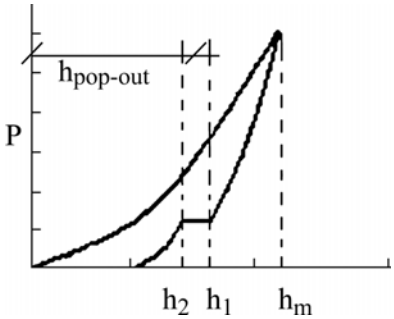

Fig. 3. Definition of indentation depths considered to characterize the occurrence of pop-out effect.

In Fig. 4 the maximum penetration depth is plotted as a function of the depth at which the "pop-out" occurred. It was very interesting to observe that the relationship between h_m and $h_{pop\text{-}out}$ is quite linear not only for Si [12] but also for the coated Si systems (Fig. 4).

It is worth noting that in all experiments the relationship between $h_{pop\text{-}out}$ and h_m is linear regardless of the conditions for the unloading rates.

DISCUSSION

The fact that the strain bursts (Fig. 2) occurred at higher loads for the coated samples was expected as the thin film coatings limit the deformation that the substrate can undergo, and in order for the "pop-out" to occur a certain amount of pressure had to be exerted on Si. Particularly, in order to deform the silicon substrate to a depth necessary for the "pop-out" effect to take place, the indenter had to overcome the mechanical resistance of the film.

The "pop-out" is affected by the unloading rate, but the $h_{pop\text{-}out}$ vs h_m relationship remains linear, and fitted lines tilt angle shows a very small variation depending on the unloading rate. This feature of the silicon "pop-out" effect can be used to study the thin films mechanical characteristics. If it is assumed that only Si can produce "pop-outs", the $h_{pop\text{-}out}$ for equal depths of deformation of Si should be the same in both uncoated and coated samples. But further studies indicated that this is not the case. Linear curves of Fig. 4 are described by the following equation:

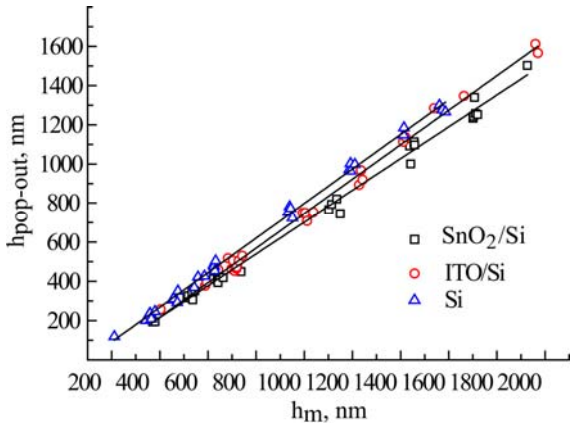

Fig. 4. $h_{pop\text{-}out}$ vs. h_m for indentation conditions of case (i): Si doped with phosphorus (substrate), as well as of ITO/Si and SnO_2/Si.

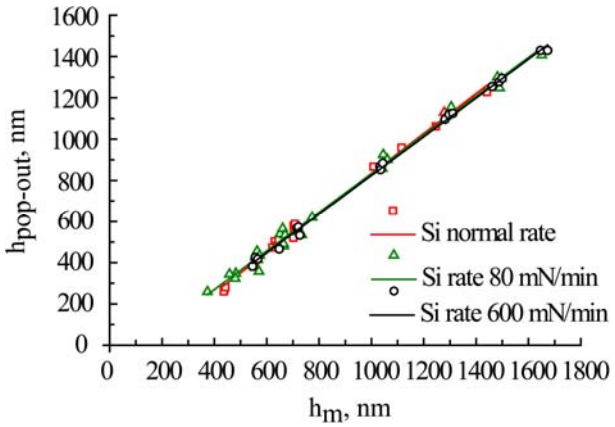

Fig. 5. $h_{pop\text{-}out}$ vs. h_m for cases (i), (ii) and (iii) for doped Si.

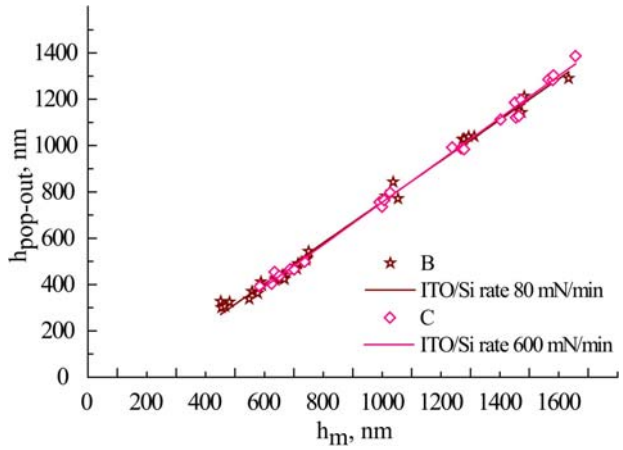

(a)

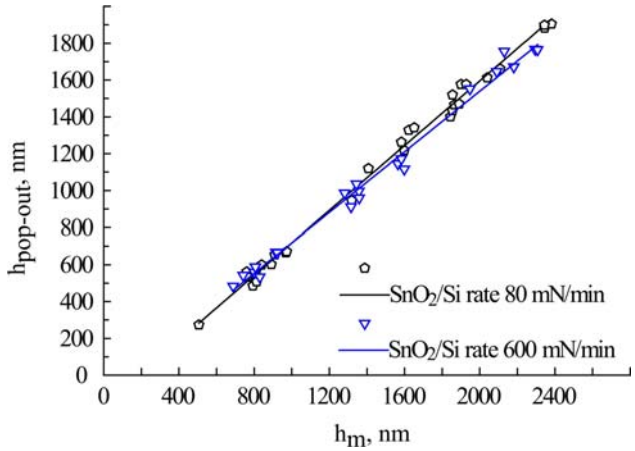

(b)

Fig. 6. $h_{pop\text{-}out}$ vs. h_m for cases (ii) and (iii) for (a) ITO/Si and (b) SnO_2/Si structures.

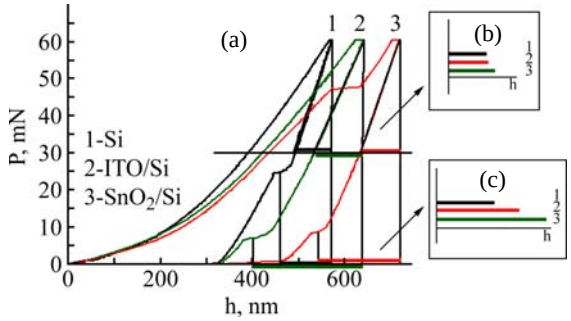

Fig. 7. (a) "Pop-out" effect when P_{max} = 60 mN for (1) Si doped with phosphorus (substrate), (2) for ITO/Si and for (3) SnO_2/Si; case (i) from Table 1; (b) indenter displacement in unloading stage for studied samples for equal time sequence; (c) $h_m - h_{pop\text{-}out}$ distance for the same applied load.

Table 3. Examples of Eq. (3).

$h_m - h_{pop\text{-}out}$, nm	Si		ITO/Si		SnO_2/Si	
	h_m, nm	$h_{pop\text{-}out}$, nm	h_m, nm	$h_{pop\text{-}out}$, nm	h_m, nm	$h_{pop\text{-}out}$, nm
270	1672	1402	1230	960	959	689
250	1450	1200	1073	823	830	580

$$h_{pop\text{-}out} = Ah_m + B \quad (2),$$

where A and B are constants which depend on Si and the coating materials properties (Table 2). The estimation of A and B is important as they allow predicting the depth at which the "pop-out" will occur once the maximum penetration depth is known. This implies that one can predict the indenter displacement depth when the phase transition (Si-II transforms into Si-XII, Si-III and α-Si mixture [27]) takes place during unloading. The physical interpretation of these constants is not clearly understood and is still being studied.

To better understand the phenomena that occur under the indenter during the unloading stage, we will examine the indentation curves for P_{max} = 60 mN (case (i) from Table 1) for all investi-

gated samples (Fig. 7a). First of all, our attention is captured by the significant difference between the maximum penetration depth in each sample. This is due to the presence of a thin film (~ 350 nm thick), which has a different Young's modulus and fracture toughness. The second difference can be observed when we compare the indenter motion speed during unloading. Fig. 7b illustrates the imprint recovery distance for the same period of time. It is interesting that in the SnO_2/Si sample the elastic recovery is faster.

The recovery process in imprints for the uncoated Si wafer is different from that of the coated systems. Even regardless of the equal unloading rates for all samples, in the uncoated Si the imprint depth decreased slower during the unloading stage. Fig. 7b presents the indenter motion distance as the indenter tip withdrew from the samples during the load decrease from 60 to 30 mN, within 15 sec (the unloading ratio is 120 mN/min according to case (i) from Table 1). The recovery speed for this case is: 5.5 nm/s for Si, 5.7 nm/s for Si covered by SnO_2 and 6.7 nm/s for Si coated by ITO. So it can be assumed that coatings (i) preserve tension in Si under the indenter and favor elastic recovery of the indented volume, (ii) delay significantly the phase transformation evolution during the unloading stage (Fig. 7c) and change the phase mixture proportions responsible for the "pop-out" effect [27] (see pop-out shape in Fig. 7a).

There appears a question: when the elastic recovery distance until the "pop-out" effect is the same in coated and uncoated Si samples? The answer may be: this will occur when the distances illustrated in Fig. 7c are equal. It is very difficult to achieve this in a "real life" experiment, but we can easily determine it from the h_m vs $h_{\text{pop-out}}$ graph of Fig. 4. We can find the distance at which the indenter had to be "removed" from the sample upon reaching the maximum depth, before the "pop-out" occurs for all of the investigated samples. An interesting observation is when

$$h_m(\text{Si}) - h_{\text{pop-out}}(\text{Si}) = h_m(\text{ITO/Si}) - h_{\text{pop-out}}(\text{ITO/Si}) = \\ = h_m(\text{SnO}_2/\text{Si}) - h_{\text{pop-out}}(\text{SnO}_2/\text{Si}). \quad (3)$$

Some results of it are presented in Table 3.

It can be clearly seen that for the same recovery depth until the "pop-out" occurred ($h_m - h_{\text{pop-out}}$) the maximum penetration depth and therefore the maximum applied load are lower in the coated systems than in the uncoated ones. The connection between recovery distance until the "pop-out" occurrence and phase transformation in Si is not clearly understood. These results indicate the difference and complexity of mechanical processes that occur in coated substrates subjected to a concentrated load action.

CONCLUSIONS

In the present study it was shown that the depth at which the strain burst ("pop-out") observed in *n*-Si, ITO/Si and SnO_2/Si during unloading strongly depends on the maximum applied load and is linearly proportional to the maximum indentation depth. In particular, the relationship of $h_{\text{pop-out}}$ vs. h_m remains linear, and the fits in Figs. 5 and 6 show a very small variation depending on the unloading rate.

Some new features of the "pop-out" effect for the coated *n*-Si structures used in photovoltaics were depicted and analyzed. It was established that the phase transformations in *n*-Si are delayed and that the phase mixture proportions responsible for the "pop-out" effect change due to the tension preservation in the imprint under the film coating. Furthermore, by comparing the indentation behavior between the ITO/Si and SnO_2/Si samples, significant differences in the mechanical properties between the two coatings can be understood.

ACKNOWLEDGEMENTS

The present study was performed in the frame of the KEA's European Research Council Starting Grant 211166 MINATRAN.

REFERENCES

1. Kriese M.D., Gerberich W.W., Moody N.R. Quantitative Adhesion Measures of Multilayer Films: Part I. Indentation Mechanics. *J Mat Res*. 1999, **14**(7), 3007–3018.
2. Gerberich W.W., Kramer D.E., Tymiak N.I., Volinsky A.A., Bahr D.F., Kriese M.D. Nanoindentation-induced Defect-interface Interactions: Phenomena, Methods and Limitations. *Acta Mat*. 1999, **47**(15), 4115–4123.
3. Kriese M.D., Boismier D.A., Moody N.R., Gerberich W.W. Nanomechanical Fracture-testing of thin Films. *Eng Fract Mech*. 1998, **61**, 1–20.
4. Volinsky A.A., Moody N.R., Gerberich W.W. Interfacial Toughness Measurements for thin Films on Substrates. *Acta Mat*. 2002, **50**, 441–466.
5. Stone D., LaFontaine W.R., Alexopoulos P., Wu T.W., Li C-Y. An Investigation of Hardness and Adhesion of Sputter-deposited Aluminum on Silicon by Utilizing a Continuous Indentation Test. *J Mater Res*. 1988, **3**(01), 141–147.
6. Pharr G.M., Oliver W.C., Clarke D.R. The Mechanical Behavior of Silicon During Small-Scale Indentation. *J Electron Mater*. 1990, **19**(9), 881–887.
7. Bradby J.E., Williams J.S., Wong-Leung J., Swain M.V., Munroe P. Transmission Electron Microscopy Observation of Deformation Microstructure under Spherical Indentation in Silicon. *Appl Phys Lett*. 2000, **77**, 3749.

8. Zarudi I., Zhang L.C., Cheong W.C.D., Yu T.X. The Difference of Phase Distributions in Silicon after Indentation with Berkovich and Spherical Indenters. *Acta Materialia*. 2005, **53**, 4795–4800.

9. Hu Huang, Hongwei Zhao, Chengli Shi, Lin Zhang, Shunguang Wan and Chunyang Geng. Randomness and Statistical Laws of Indentation-Induced Pop-Out in Single Crystal Silicon. *Materials*. 2013, **6**(4), 1496–1505.

10. Gerk A.P., Tabor D. Indentation Hardness and Semiconductor-metal Transition of Germanium and Silicon. *Nature*. 1978, **271**, 732–733.

11. Zarudi I., Zou J., Zhang L.C. Microstructures of Phases in Indented Silicon: A High Rezolution Characterization. *Appl Phys Lett*. 2003, **82**(6), 874–876.

12. Grabko D.Z., Harea E.E. "Pop-out" Effect in ITO/Si and SnO_2/Si Structures. *Surf Eng Appl Electrochem*. 2013, **49**(1), 36–41.

13. Yan J.W., Takahashi H., Gai X.H., Harada H., Tamaki J., Kuriyagawa T. Load Effects on the Phase Transformation of Single-crystal Silicon During Nanoindentation Tests. *Mater Sci Eng*. A. 2006, **423**, 19–23.

14. Bradby J.E., Williams J.S., Wong-Leung J., Swain M.V., Munroe P. Mechanical Deformation in Silicon by Micro-indentation. *J Mater Res.* 2001, **16**(5), 1500–1507.

15. Domnich V., Gogotsi Y., Dub S. Effect of Phase Transformations on the Shape of the Unloading Curve in the Nanoindentation of Silicon. *Appl Phys Lett*. 2000, **76**(16), 2214–2216.

16. Liu Y.H., Chen T.C., Yang P.F., Jian S.R., and Lai Y.S. Atomic-level Simulations of Nanoindentation-induced Phase Transformation in Mono-crystalline Silicon. *Appl Surf Sci*. 2007, **254**, 1415–1422.

17. Rao R., Bradby J.E., Williams J.S. Patterning of Silicon by Indentation and Chemical Etching. *Appl Phys Lett.* 2007, **91**(12), 123113.

18. Simashkevich A.V., Sherban D.A., Bruk L.I., Kharya E.E. and Usatii Iu. Efficient ITO/nSi Solar Cells with Silicon Textured Surface. *Surf Eng Appl Electrochem*. 2011, **47**(3), 266–271.

19. Yin Zhi Chen, Hong Chuan Jiang, Shu Wen Jiang, Xing Zhao Liu, Wan Li Zhang. Thin Film Thermocouples for Surface Temperature Measurement of Turbine Blade. *Advanced Materials Research.* 2014, **873,** 420–425.

20. Kai Wah Yeung, Chung Wo Ong. Micro-pressure Sensors Made of Indium tin Oxide thin Films. *Sensors and Actuators A.* 2007, **137,** 1–5.

21. Otto J. Gregory and Tao You. Piezoresistive Properties of ITO Strain Sensors Prepared with Controlled Nanoporosity. *J Electrochem Soc.* 2004**,** **151**(8), H198–H203.

22. Simashkevich A., Sherban D., Bruc L., Coval A., Fedorov V., Bobeico E. and Usatii Iu. Spray Deposited ITO/nSi Solar Cells with Enlarged Area. *Proc. of the 20th European Photovoltaic Solar Energy Conference*. Barcelona, Spain. 2005, pp. 980–982.

23. ISO 14577-4: *Test Method for Metallic and Non-metallic Coatings*.

24. Oliver W.C. and Pharr G.M. Measurement of Hardness and Elastic Modulus by Instrumented Indentation: Advances in Understanding and Refinements to Methodology. *J Mater Research*. 2004. **19**(1): p. 3–20.

25. Rosenfeld L.G., Ritter J.E., Lardner T.J., Lin M.R. Use of the Microindentation Technique for Determining Interfacial Fracture Energy. *J Appl Phys*. 1990, **67**(7), 3291–3296.

26. Fischer-Cripps A. *Nanoindentation*. *Mechanical Engineering Series 1*. Springer Science+Business Media, LLC 2011, 304 p.

27. Juliano T., Gogotsi Yu, and Domnich V. Effect of Indentation Unloading Conditions on Phase Transformation Induced Events in Silicon. *J Mater Res*. 2003, **18**(5), 1192–1201.

Received 05.03.14
Accepted 19.06.14

Реферат

Наиболее интересным явлением, замеченным в наноиндентировании кремния, считается разрыв деформационной кривой на стадии разгрузки. Данная особенность названа «pop-out» эффектом и относится к фазовым превращениям, имеющим место под индентором при большом давлении. Одним из свойств данного эффекта является обнаруженная нами линейная зависимость между глубиной, на которой «pop-out» эффект, и максимальной глубиной проникновения индентора. Систематическое изучение легированного Si, а также фотопреобразователей типа ITO/Si и SnO_2/Si показало, что данная линейность сохраняется при разных скоростях разгрузки индентора, которые сильно влияют как на появление «pop-out» эффекта, так и на контактное давление. Более того, показано, что фазовые превращения в легированном кремнии, покрытом тонкой плёнкой, заторможены из-за сохранения механического напряжения в отпечатке под пленкой. Эти наблюдения предполагают необходимость дальнейших исследований механических свойств на границе раздела между плёнкой и кремниевой подложкой в плёночных структурах (МЭМС и ФЭП).

Ключевые слова: «pop-out» эффект, кремний, наноиндентирование, кремниевая структура, фотопреобразователи.